ICAS 2016
30th Congress of the International Council of the Aeronautical Sciences
DCC, Daejeon, Korea ; September 25-30, 2016

LARGE-SCALE VORTEX STRUCTURE OF FLOW IN THE NEAR WAKE BEHIND AN AIRLINER DURING TAKEOFF AND LANDING

Yu.M. Tsirkunov*, M.A. Lobanova*, A.I. Tsvetkov, B.A. Schepanyuk****
***Baltic State Technical University, Saint Petersburg, Russia**
****Centre of Applied Aerodynamics, Research Park, Saint Petersburg State University**

Keywords: *cruising aircraft, takeoff and landing, near wake, computational simulation PIV-measurements*

Abstract

The large-scale flow vortex structure in the near-field wake of airliner moving on the runway during its takeoff and landing was investigated numerically on the basis of RANS approach with the SST turbulence model using ANSYS soft. Numerical results are compared with the ones obtained earlier for a cruising flight, and they are added by experimental data in the wind tunnel.

1 Introduction

Civil aviation is an essential element of contemporary global society. A permanently increase of a number of air passengers and an airlift tonnage results in an increase of frequency of aircraft takeoff and landing at airports. An aircraft accelerating on the runway or landing generates a long-living large-scale vortex flow behind it which is known as a vortex wake. Such a wake behind a large airliner, presents a serious danger for a following aircraft, and this limits a runway capacity. For the safety of takeoff, cruising flight and landing it is critically important to predict the wake properties, particularly its large-scale vortex structure. Also it is important to develop methods of wake vortices break-down. A great number of publications deals with the study of the aircraft wake for a cruising flight (see, e.g., [1, 2] and numerous references in these books). The problem of wake vortices shed by commercial aircrafts is discussed in excellent paper [3] which gives a consolidated European view on the status of knowledge on the nature and characteristics of aircraft wakes. However a very few papers are dedicated to the vortex flow structure behind an aircraft during takeoff and landing (e.g., [4]).

In the present paper, the large-scale vortex structure of the wake behind an aircraft moving along the runway during both takeoff and landing is investigated numerically. The aircraft speed in calculations corresponded to that when the nose wheel lift-off during takeoff or the touchdown during landing. The main attention is paid to the effects of the trailing-edge flaps and spoilers position on the near-field wake flow.

Special experiments were also carried out in the wind tunnel for measurements of flow parameters in the wake of an aircraft model near the flat plate which played the role of a runway. Experimental part of this work served for validation of the flow model used in computations.

2 Geometrical Configuration of an Aircraft

The configuration of an aircraft for numerical study and physical experiments was taken like Boeing 737-300. The aircraft 3D geometrical model was designed using SolidWorks15. It included all essential elements: a body (fuselage), wings with winglets, horizontal and vertical stabilizers, engine nacelles, nacelle pylons, inboard flap track fairings, Krueger flaps, slats, trailing-edge flaps, flight and ground spoilers. Krueger flaps and slats were fully extended for both takeoff and landing. The

trailing-edge flap position was different for takeoff and landing conditions: 15 and 40 units respectively. Spoilers were up-deflected only for the landing condition. Coordinates of airfoils in various wing cross-sections were taken from UIUC Airfoil Coordinates Database [5]. Aircraft sizes were taken from available in the open information sources [6]. The body length was 32.2 m, wing span with winglets was 31.2 m, body height and width in the middle part were 4.01 m and 3.76 m, respectively, wing dihedral was 6°, horizontal stabilizer span was 12.7 m, horizontal stabilizer dihedral was 7°, angle between the root airfoil chord and the body centerline (setting angle) was +1°, the wing was geometrically twisted and the setting angle for wing tip was –0.8°. The horizontal stabilizer had no geometrical twisting and its setting angle was –2°. Configuration and sizes of the engine were taken close to the turbofan engine CFM 56-3. The length of the engine nacelle was 4.0 m. The diameters of the annular exhaust duct and bypass duct outlets were 0.51 and 0.76 m, and 1.04 and 1.30 m, respectively. The general aircraft configuration is shown in Figs. 1 and 2.

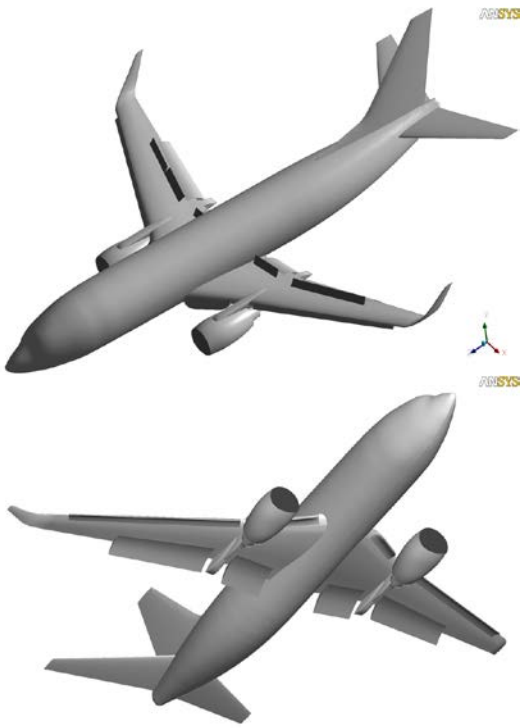

Fig. 1. General view of the aircraft model with the leading- and trailing-edge flaps, and spoilers position corresponding to the landing conditions.

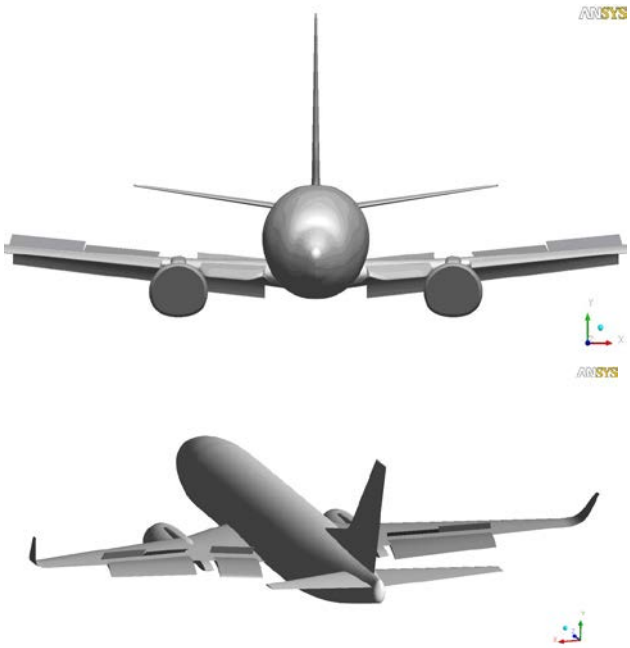

Fig. 2. Front and back view of the aircraft model with the leading- and trailing-edge flaps, and spoiler's position corresponding to the landing conditions.

3 Flow Model

The Reynolds number of flow over an aircraft is high (~10^8), and hence the flow is turbulent. It was described by the Reynolds averaged Navier–Stokes equations with Menter k–ω SST turbulence model [7] which gives a good agreement with the experimental data in drag and lift force coefficients for the simplified aircraft model configuration (wing/body and wing/body/nacelle/pylon) [8]. This flow model, as any other RANS-based model, does not allow us to resolve the small-scale turbulent vortices, but it is quite applicable for studying the large-scale vortex flow structure. Calculations were performed with the use of ANSYS soft.

4 Calculation Domain, Grid and Boundary Conditions

The calculation domain represented a rectangular parallelepiped (see Fig. 3) with 160.9 m length (5 body lengths), 46.7 m width (approx. wing semispan plus body length), and 34.8 m height (approx. body length). The forward point of the fuselage was located at the distance of 32.2 m (body length) from the inlet boundary. Directions of coordinate axes are

shown in Fig. 3 (z-axis is pointed in the opposite direction to the free stream velocity vector). The flow over an aircraft was assumed to be symmetric relative to the vertical plane passing through the aircraft centerline. The origin of the coordinate system is located in the plane of symmetry at the distance of 28.9 m from the inlet boundary and 2.6 m from the bottom boundary (runway). Directions of coordinate axes are shown in Fig. 3. The outlet boundary is located at z_{out} = –132.0 m. An unstructured all boundary-fitted (included aircraft surface) grid was designed using the ANSYS ICEM CFD soft. At first, the surface grid on the aircraft was constructed, then it was fixed and a volume grid was generated in the calculation domain. The total number of cells of the volume grid was approximately 11.2 million for takeoff and 12.5 million for landing conditions. The grid was refined towards the aircraft surface, and in the wake area.

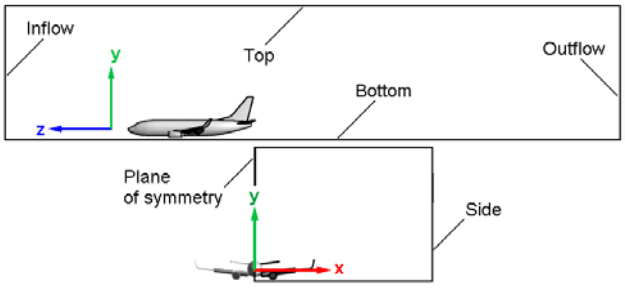

Fig. 3. Calculation domain and aircraft position: side view (top) and front view (bottom).

At the inlet boundary, the velocity vector was taken as normal to it, and the temperature and total pressure were specified as follows: T = 288.15 K, p_0 = 104357.6 Pa. These values corresponded to the free stream velocity V = 70 m/s (this is the aircraft speed on the runway) and static pressure p = 101325 Pa. Such a technique gave the entropy distribution at the inlet boundary very close to uniform (the difference between maximal and minimal values of the static entropy was much less than in the case of traditional specification of the velocity vector and the static pressure) that is physically correct. This technique is similar to that used in calculations of flow through a cascade of airfoils. The turbulence intensity was taken equal to 0.001.

At the outlet boundary, the free stream pressure (p = 101325 Pa) was imposed, all other parameters were extrapolated from the calculation domain.

The boundary conditions at the top and side boundaries were specified as 'opening' with the following velocity vector components and the temperature V_x = 0; V_y = 0; V_z = –70 m/s, T = 288.15 K; the turbulent intensity was 0.001.

Zero normal-velocity component together with the 'no-sleep wall' and adiabatic conditions were imposed at the aircraft surface.

The bottom boundary (runway) was considered as moving wall, and gas velocity components at it were taken as at the top or side boundaries. All surfaces with “wall” boundary condition were assumed to be smooth and adiabatic.

The conditions of symmetry were specified at the plane of symmetry: the normal velocity (x-component) and all derivatives of thermodynamic parameters and y- and z-components of the velocity vector with respect to the normal direction (x-direction) were zero. These conditions are valid if the crosswind is absent.

In calculations (not in experiments), the engines were considered as operating, and the gas velocity and temperature at the exit of the exhaust nozzle (V_1 and T_1) and the bypass duct (V_2 and T_2) were found from preliminary thermodynamic calculations of the turbofan engine CFM 56-3. They were found to be the following: V_1 = 517.37 m/s, T_1 = 883.36 K, and V_2 = 366.86 m/s, T_2 = 288.15 K. The turbulence intensity was taken 5 %. For simplicity, the gas constant and the ratio of specific heats for combustion products were taken identical to those for air. It is rather rough assumption, but it allowed us not to simulate in detail the processes of mutual diffusion and mixing of the combustion products with the cocurrent air flow.

The free stream velocity vector, temperature and pressure were taken as the initial conditions in the whole calculation domain for solving the time-dependent RANS, equations.

Steady-state flow in the wake was obtained as the limit of time-dependent solution.

5 Experimental Setup and PIV system

Experimental study of wake flow was carried out at the Centre of Applied Aerodynamics of Saint Petersburg State University. The aircraft model was made on 3D printer in the scale 1:66 relative to the aircraft size used in computational simulation, but engines were made as a contoured ducts (see Fig. 4).

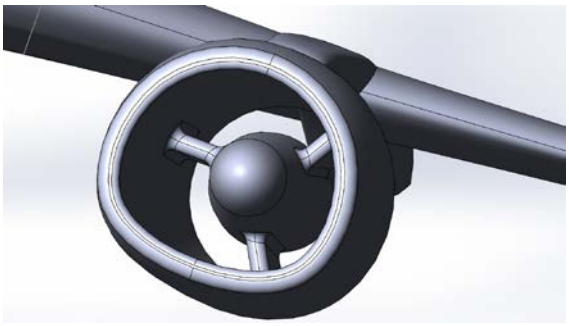

Fig. 4. Configuration of an engine duct in experiments.

The model was placed in the center of the open test section of the wind tunnel AT-11 near the glass screen (model of a runway) as it is shown in Fig 5. It was positioned at the distance of 16 mm from the surface of a and 151 mm from its leading edge. The diameter and length of the test section was 2.25 m and 4 m, respectively.

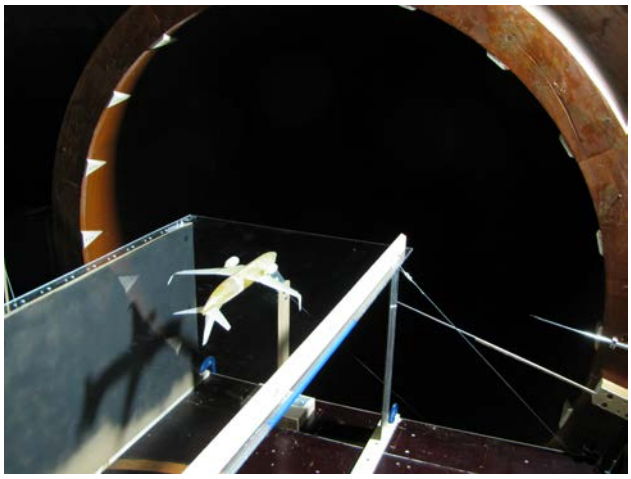

Fig. 5. View of an aircraft model in the test section.

PIV system was used for measurement of the velocity field in the aircraft wake. This system included double-pulse NdYAG laser Quantel Twins CFR300, focusing lens Nikkor ED-180 mm with focal lenth 180 mm, cross-correlation camera Videoscan-11002, timing sync processor, fog generation Magnum ZR33, three-axis traverse and control system. The camera had a matrix KAI-11002M with CCD size 36x24 mm and image resolution 4000x2673 px. Airflow seeding was carried out using a fog generator filled with a hydroglyceric blend 'MT Solid Fog Dense' giving 0.1…5 μm particle size. Time interval between two flashes of double-pulse laser was $\Delta t = 22$ μs. At each plane of measurements in the wake, 200 instantaneous velocity fields were recorded by optical recording system to provide high accuracy of measurements. The results were processed with ActualFlow software.

6 Results and Discussion

The main aim of present study was to investigate the large-scale vortex structure of the wake flow in two cases: an aircraft runs on a runway during takeoff and landing. The Krueger flaps and slats are in both cases at the same position (they are fully extended), but positions of trailing-edge inboard and outboard flaps and spoilers are quite different. The trailing-edge flaps are at the position of 15 units for takeoff and 40 units for landing. The flight and ground spoilers do not work during takeoff, but they are fully declined during landing.

In the last case, the wake flow is disturbed more strongly. Streamlines obtained in computational simulation are shown in Fig. 6.

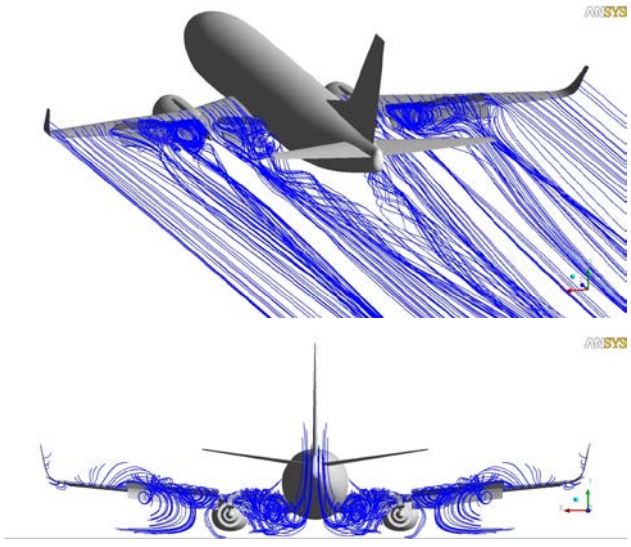

Fig. 6. General view (top) and back view (bottom) of streamlines behind an aircraft during landing.

Fields of z-component (see Fig. 3 for notation of coordinate axes) of the vorticity, and corresponding to them kinematic patterns (arrows show the direction of circulation flow) in four cross-sections for takeoff and landing conditions are shown in Figs. 7 and 8 (left parts of pictures are obtained by mirror reflection of right parts). Two large vortices are clearly seen on both sides, they rotate in the opposite directions, and their intensity being rather high just behind an aircraft decreases quickly with distance from an aircraft. The intensity of each vortex at the landing conditions is much higher than at the takeoff conditions.

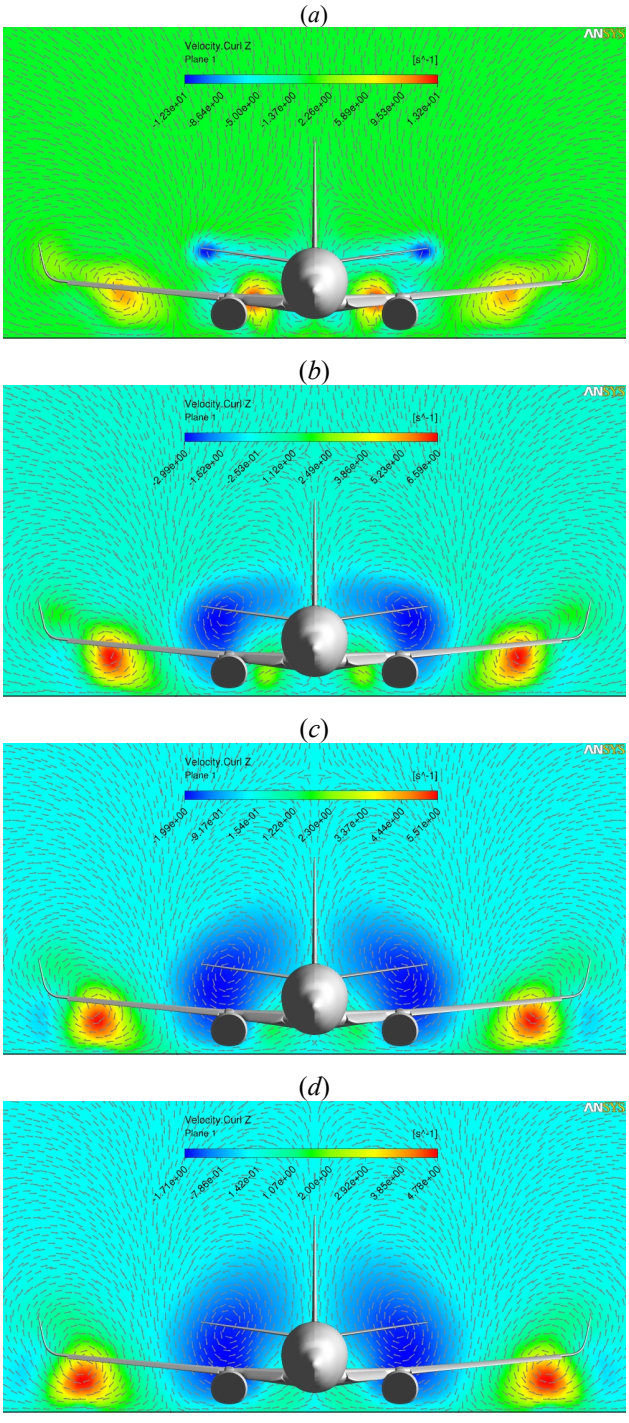

Fig. 7. Field of z-component of vector curl **V** and velocity plots behind an aircraft running on a runway during takeoff: (*a*) z = –40 m, (*b*) –70 m, (*c*) –100 m, (*d*) –130 m. Scale on each picture is local and related to the right part.

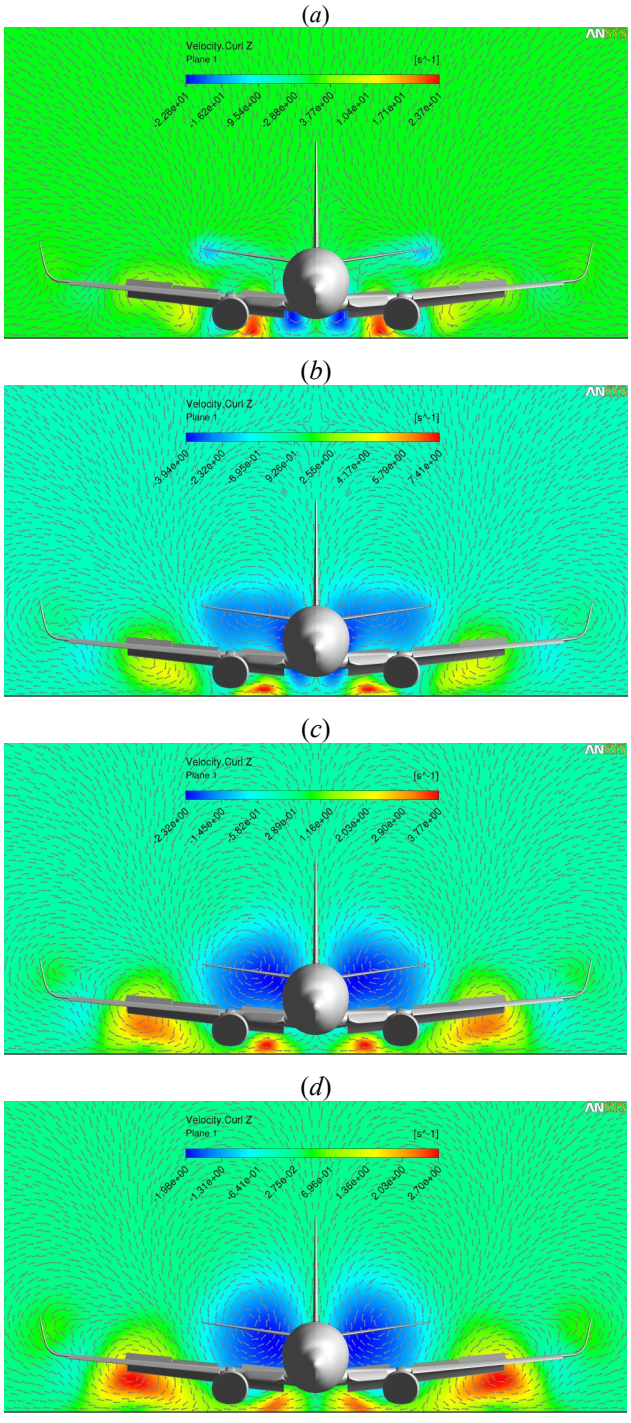

Fig. 8. Field of z-component of vector curl **V** and velocity plots behind an aircraft running on a runway during landing: (*a*) z = –40 m, (*b*) –70 m, (*c*) –100 m, (*d*) –130 m. Scale on each picture is local and related to the right part.

Another flow parameter which is of great interest in the considered problem is the turbulence intensity. Fields of the turbulent kinetic energy in flow cross-sections at different distance from the aircraft are shown in Figs. 9 (takeoff) and 10 (landing). It is seen that the level of turbulence in the wake is determined mainly by exhaust jets. The effect of flaps and spoilers is low. In both cases jets approach each other with distance from the aircraft. This is also demonstrated by the view of jet streamlines (see Fig. 11). It is interesting to note that exhaust jets in the near wake in the case of cruising flight move apart [9] (see Fig. 12).

(*a*)

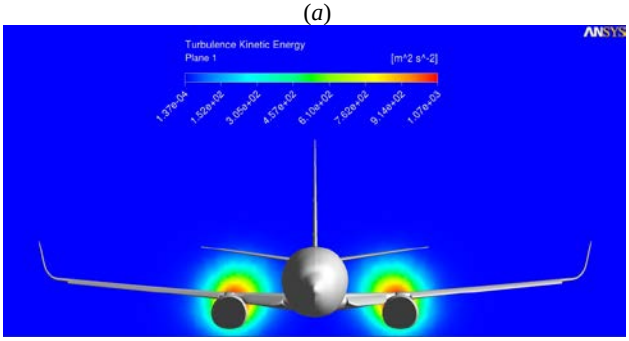

(*b*)

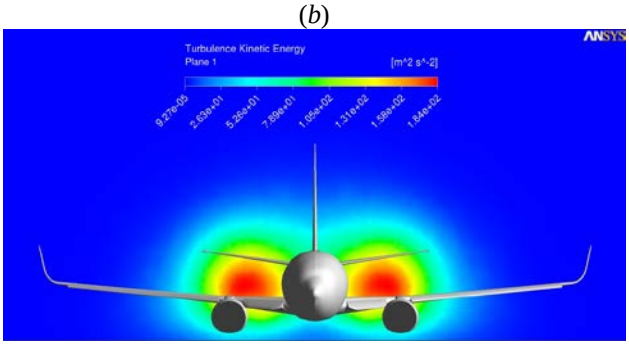

(*c*)

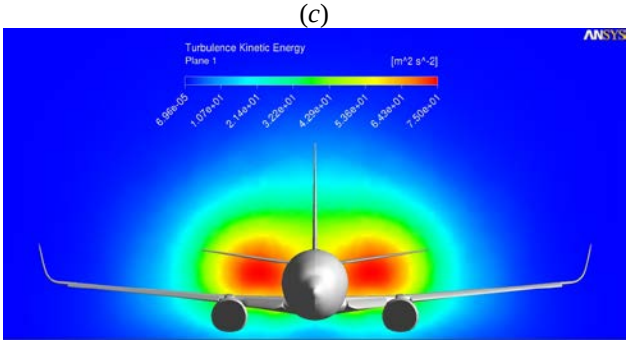

(*d*)

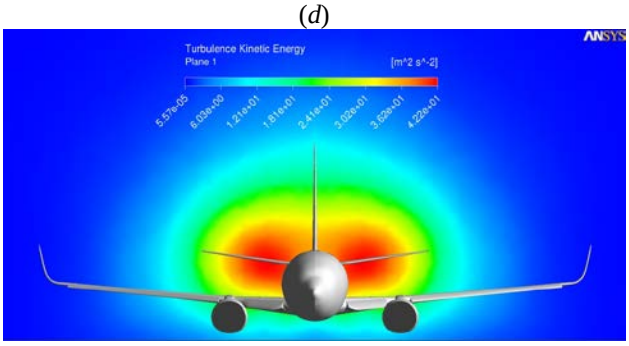

Fig. 9. Field of the turbulent kinetic energy behind an aircraft running on a runway during takeoff: (*a*) z = –40 m, (*b*) –70 m, (*c*) –100 m, (*d*) –130 m. Scale on each picture is local.

(*a*)

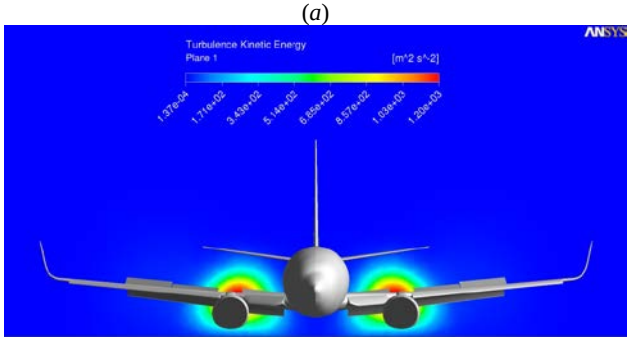

(*b*)

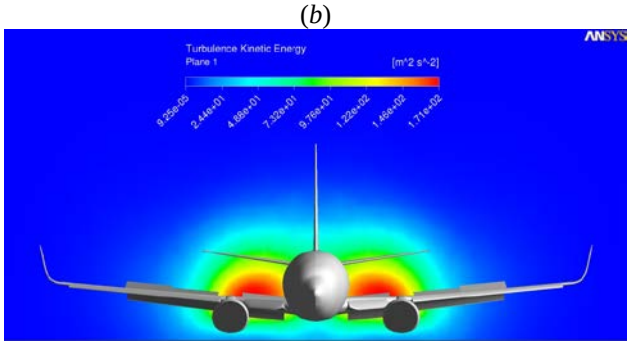

(*c*)

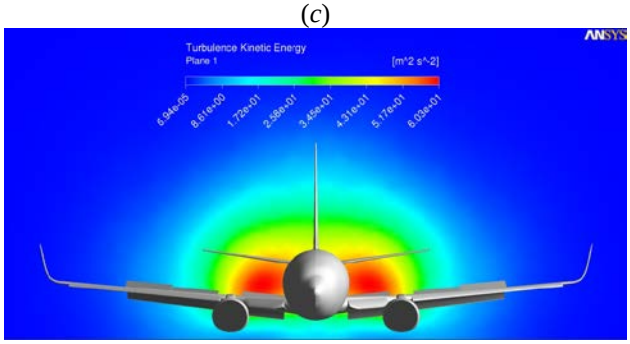

(*d*)

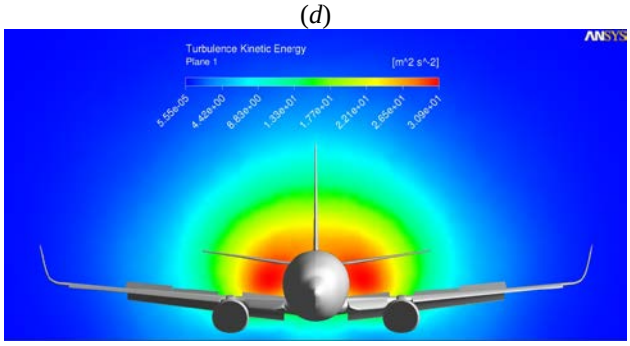

Fig. 10. Field of the turbulent kinetic energy behind an aircraft running on a runway during landing: (*a*) z = –40 m, (*b*) –70 m, (*c*) –100 m, (*d*) –130 m. Scale on each picture is local.

Fig. 11. Back view of existing jets from exhaust nozzle (red) and bypass duct (yellow).

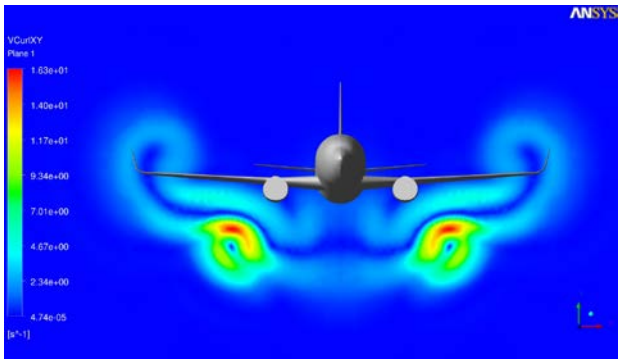

Fig. 12. Field of (xy)-component of the vector curl **V** demonstrating moving apart of jets (red-yellow areas) during the cruising flight: z = – 130 m [9].

The substantial difference between the intensity of large-scale vortices in the wake at takeoff and landing conditions is demonstrated by plots of the vertical velocity along the line $y = 0$ (Fig. 13) at fixed z. These plots have several peaks. The maximal value of the velocity for landing is approximately twice as large as that for takeoff. This is caused by quite different positions of flaps and spoilers in these cases. The largest difference between maximal and minimal vertical velocities at $y = 0$ in the wake cross-section is observed just behind an aircraft: it reaches 12 m/s at takeoff and 17 m/s at landing conditions. This difference decreases with distance from an aircraft, and becomes about 5 m/s at $z = -130$ m (3 fuselage lengths behind an aircraft). In the case of cruising flight it can reach 28 m/s just behind an aircraft and remains rather high (approx. 20 m/s) at the distance of 3 fuselage lengths [9].

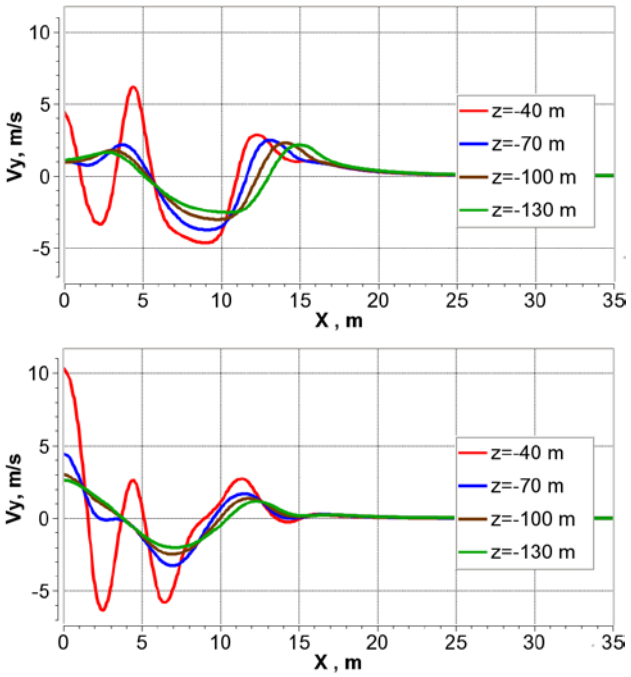

Fig. 13. Vertical velocity as a function of x along the line $y = 0$ at different z in the wake for takeoff (top) and landing (bottom) conditions.

Distribution of the vertical velocity along the line $y = 0$ was also measured in wind tunnel experiments (see. Sec. 5). Outer envelopes of models in numerical simulation and in experiments were geometrically similar to each other, however air-gas channel inside the engine was different. Mach and Reynolds numbers in these cases were also different. The free stream velocity in experiments was 20 m/s (in computational simulation it was 70 m/s). The plot of function obtained in experiment for the landing aircraft model configuration at the distance of 1/5 of the fuselage length behind an aircraft is shown in Fig. 14. In spite of a rather strong difference of flow parameters, the character of variation of V_y with x in experiment is identical to that in numerical calculations (cf. with red curve in Fig. 13, bottom).

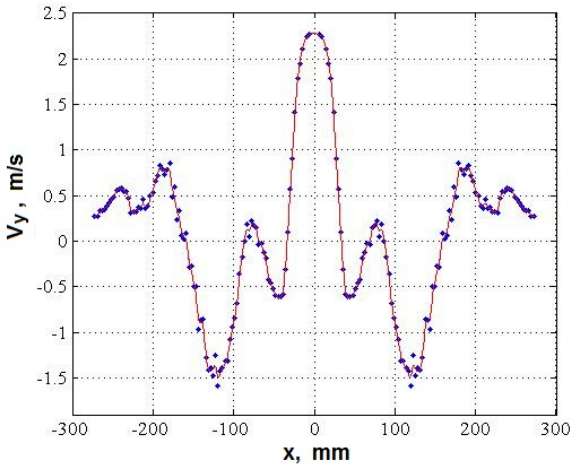

Fig. 14. Experimental distribution of V_y with x.

7 Concluding Remarks

The present paper describes rather work in the progress than a completed study. Additional computational investigation and experiments have to be carried out for estimation of both numerical and physical flow patterns and flow fields. Nevertheless, the present results demonstrate many important features of the large-scale near-field wake flow structure behind an aircraft during its takeoff and landing.

8 Acknowledgments

This work was supported by the Russian Foundation for Basic Research through grant No. 15-08-07965. The authors also thank Dr. A. Karpenko for making PIV measurements and V. Gabdylkhakova for PIV data processing.

References

[1] Ginevsky A.S. and Zhelannikov A.I. *Vortex wakes of aircrafts*. Fizmatlit, Moscow, 2008. [in Russian]

[2] Gaifullin A.M. *Vortex flows*. Nauka, Moscow, 2015. [in Russian]

[3] Gerz Th., Holzapfel F. and Darracq D. Commercial aircraft wake vortices. *Progress in Aerospace Sciences*, Vol. 38, pp. 181-208, 2002.

[4] Stephan A., Holzapfel F., Misaka T. Simulation of aircraft wake vortices during landing with decay enhancing obstacles. *Proc. of 29th Congress of the Int. Council of the Aeronautical Sciences (ICAS 2014)*, St. Petersburg, Russia, paper No. 2014_0796, pp. 1-10, 2014.

[5] http://www.ae.illinois.edu/m-selig/ads/coord database.html

[6] http://www.b737.org.uk/

[7] Menter F.R. Two-equation eddy-viscosity turbulence models for engineering applications. *AIAA Journal*, Vol. 32, pp. 1598-1605, 1994.

[8] Menter F.R., Kuntz M. and Langtry R. Ten years of industrial experience with the SST turbulence model. *Turbulence, Heat and Mass Transfer 4* (Eds.: K. Hanjalic, Y. Nagano M. Tummers). Begell House, 2003.

[9] Lobanova M.A., Tsirkunov Y.M. Numerical simulation of a jet-vortex wake behind a cruise aircraft. *Proc. 6th European Congress on Computational Methods in Applied Sciences and Engineering (ECCOMAS 2012), Vienna, Austria*, paper No. 1823, pp. 1-14, 2012.

8 Contact Author Email Address

mailto: Yury-Tsirkunov@rambler.ru

Copyright Statement